Acta Crystallographica Section D
Biological Crystallography
ISSN 0907-4449

A neutron crystallographic analysis of phosphate-free ribonuclease A at 1.7 Å resolution

Daichi Yagi,[a] Taro Yamada,[b] Kazuo Kurihara,[c] Yuki Ohnishi,[d] Masahiro Yamashita,[a] Taro Tamada,[c] Ichiro Tanaka,[d] Ryota Kuroki[c] and Nobuo Niimura[b]*

[a]Graduate School of Science and Engineering, Ibaraki University, Hitachi 316-8511, Japan, [b]Frontier Research Center of Applied Atomic Sciences, Ibaraki University, Tokai 319-1106, Japan, [c]Japan Atomic Energy Agency, Tokai 319-1184, Japan, and [d]Faculty of Engineering, Ibaraki University, Hitachi 316-8511, Japan

Correspondence e-mail: niimura@mx.ibaraki.ac.jp

Received 5 February 2009
Accepted 19 May 2009

PDB Reference: ribonuclease A, 3a1r, r3a1rsf.

A neutron crystallographic analysis of phosphate-free bovine pancreatic RNase A has been carried out at 1.7 Å resolution using the BIX-4 single-crystal diffractometer at the JRR-3 reactor of the Japan Atomic Energy Agency. The high-resolution structural model allowed us to determine that His12 acts mainly as a general base in the catalytic process of RNase A. Numerous other distinctive structural features such as the hydrogen positions of methyl groups, hydroxyl groups, prolines, asparagines and glutamines were also determined at 1.7 Å resolution. The protonation and deprotonation states of all of the charged amino-acid residues allowed us to provide a definitive description of the hydrogen-bonding network around the active site and the H atoms of the key His48 residue. Differences in hydrogen-bond strengths for the α-helices and β-sheets were inferred from determination of the hydrogen-bond lengths and the H/D-exchange ratios of the backbone amide H atoms. The correlation between the B factors and hydrogen-bond lengths of the hydration water molecules was also determined.

1. Introduction

Bovine pancreatic ribonuclease A (RNase A) is a major ribonuclease in the bovine pancreas which cleaves and hydrolyzes RNA exclusively at pyrimidine nucleoside positions. RNase A consists of 124 amino acids, has a mass of about 14 kDa and an isoelectric point of pH 9.6 and is a comparatively stable protein. The structure was initially solved by X-ray diffraction analysis at 5.5 Å resolution (Avey *et al.*, 1967). Subsequently, a high-resolution (1.05 Å) X-ray diffraction analysis of RNase A was carried out at six different pH values and several results related to H atoms were proposed, such as (i) the protonation states of His12, (ii) the conformational changes of His119 and (iii) the pH-dependent nature of the hydrogen-bonding network around residue His48 caused by significant pH-dependent movement of Gln101 (Berisio *et al.*, 1999, 2002).

The mechanism of the cleavage reaction catalyzed by RNase A involves two key histidine residues: His12 and His119 (Findley *et al.*, 1961, 1962; Park *et al.*, 2001). In the transphosphorylation reaction, His12 acts as a base to abstract a proton from the 2′-hydroxyl group of a ribose ring, while His119 acts as an acid to donate a proton to the 5′-oxygen of the leaving group (Fig. 1*a*). The roles of His12 and His119 as base and acid are switched in the subsequent hydrolysis reaction of 2′,3′-cyclic nucleotide substrates (Fig. 1*b*). It is important to know the protonation states of His12 and His119

in order to understand the hydrolysis mechanism of ribonuclease A. Neutron protein crystallography can contribute significantly towards solving problems such as this. In principle, it is a powerful technique that is capable of providing information on all the hydrogen atomic positions and the hydration structure around a protein; this in turn allows us to discuss not only the roles of individual H atoms and water molecules, but also of hydrogen bonds in which the positions of the H atoms are explicitly included. Hydrogen bonds in proteins are very important because the stability of the folded structure and the physiological functions of an enzyme are often correlated with the positions of hydrogen bonds and, in many cases, the formation of water-molecule networks by hydrogen bonds. H atoms play an important role in the physiological functions of many enzymes involved in hydrolysis and dehydrogenation and in some cases also oxidation–reduction.

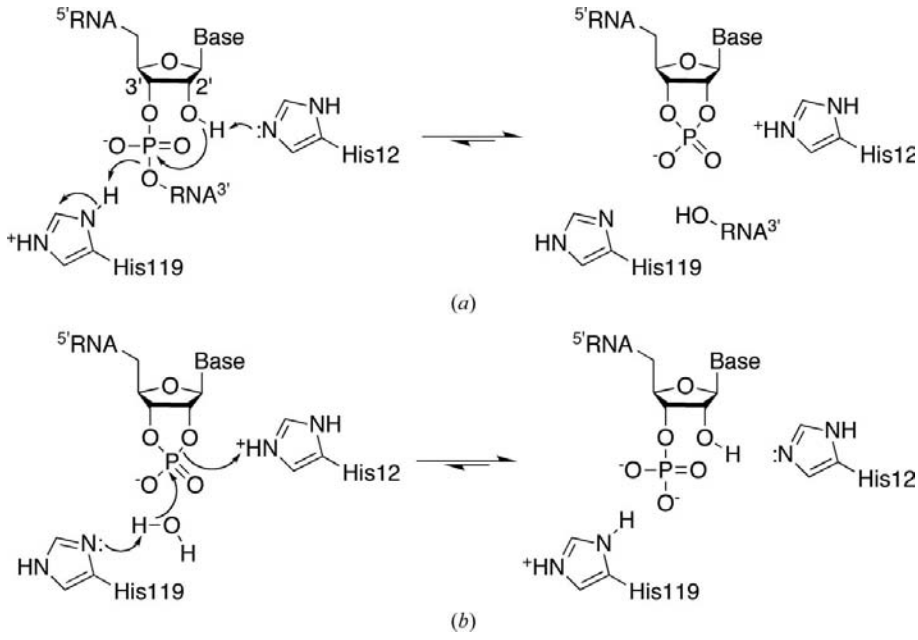

Figure 1
Putative mechanism of catalysis by ribonuclease A. (*a*) Transphosphorylation reaction. (*b*) Hydrolysis reaction (Park *et al.*, 2001).

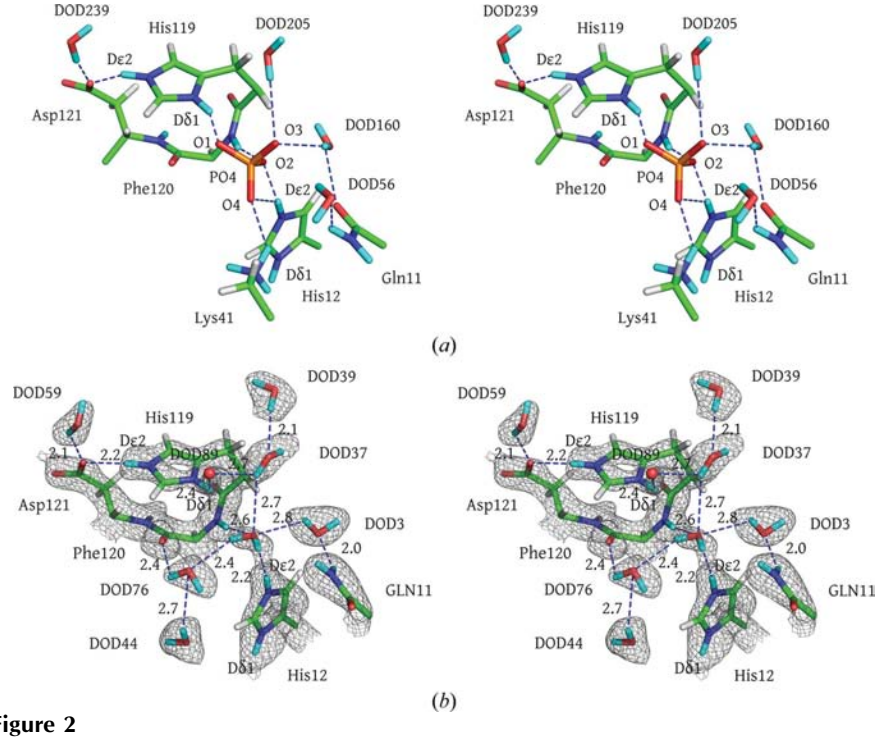

Figure 2
(*a*) Active site of RNase A complexed with a phosphate group drawn using the atomic coordinates from PDB entry 5rsa (Wlodawer *et al.*, 1986). (*b*) Active site of phosphate-free RNase A (this study). The grey mesh shows the $2|F_o| - |F_c|$ nuclear density map at the 1.3σ level. Potential hydrogen bonds are indicated by blue broken lines.

In previous publications, two structures of RNase A complexed with a phosphate ion and uridine vanadate, the latter of which is a transition-state analogue, have been determined by neutron diffraction analysis (Wlodawer, 1980; Wlodawer *et al.*, 1983, 1986; Wlodawer & Sjölin, 1983). It was reported that the phosphate group is hydrogen bonded to His12 and His119, which were both found to be doubly protonated as shown in Fig. 2(*a*), which is drawn according to the atomic coordinates from PDB entry 5rsa (Wlodawer *et al.*, 1986), even though single protonation of His12 is adequate for catalytic activity (Usher *et al.*, 1972; Lindquist *et al.*, 1973). It was further proposed that Lys41 might aid in the deprotonation of the 2′-hydroxyl group prior to the formation of a 2′,3′-cyclic intermediate. In their model, $D^{\zeta 3}$ of Lys41 is hydrogen bonded to the phosphate O4 atom. Another possible interpretation is that in the initial phosphate-free state His12 might not be doubly protonated but that later, during the formation of a complex structure (a phosphate-bound model) with a negatively charged phosphate group to fulfil the second step of the enzymatic reaction as shown in Fig. 1(*b*), a doubly protonated state of His12 is formed. In order to shed further light on this hypothesis, we carried out a neutron diffraction experiment on RNase A to determine the structure of the initial state without a phosphate group at the highest resolution possible. We succeeded in obtaining a structural model for bovine pancreatic RNase A at 1.7 Å resolution.

2. Material and methods

2.1. Crystallization

Bovine pancreatic RNase A (type XII-A) was purchased from Sigma–Aldrich Co. (R5500, Lot 052K7676). A 50% aqueous solution of *t*-butyl alcohol was poured gently onto lyophilized RNase A. The final concentration of RNase A was 4 mg ml^{-1}. The mixture was kept at 293 K. The crystal grew to 14 mm^3 (4.0 × 2.2 × 1.6 mm) after a week; its size was highly suitable for neutron diffraction experiments. Thereafter, the crystal was soaked in deuterated solution at pD 6.2 for two months to reduce background scattering from H atoms, which have a large incoherent neutron scattering length. The pD of the soaking solution was estimated by adding 0.4 units to the apparent pH, which was measured using a Horiba D-50 pH meter. The crystal was mounted in a sealed quartz capillary of 3 mm in diameter.

2.2. Data collection and refinement

RNase A crystallized in the monoclinic space group $P2_1$, with unit-cell parameters a = 30.38, b = 38.56, c = 53.40 Å, β = 105.78°. The neutron diffraction experiment was carried out at room temperature using the BIX-4 single-crystal diffractometer installed at the JRR-3 reactor of the Japan Atomic Energy Agency (Niimura *et al.*, 1994, 2006; Tanaka *et al.*, 1999, 2002). A step-scanning method with an interval of 0.3° was used to collect data, with an exposure time of 30 min per frame. After collecting 608 frames, the crystal rotation axis was changed by about 90° to a different rotation axis and 603 more frames were collected. The intensities of the reflections were integrated and scaled using the programs *DENZO* and *SCALEPACK* (Otwinowski & Minor, 1997). The statistics of the data reduction and the structure refinement are summarized in Table 1. The geometrical restrictions of the rectangular detector, which allowed the measurement of 1.4 Å data in the horizontal plane but only 2.6 Å data in the vertical direction, restricted the completeness of the high-resolution data. This meant that although two crystal orientations were used, the outermost shell (1.45–1.40 Å) has only 20% completeness. Nevertheless, this shell has significant diffraction with an average $I/\sigma(I)$ of 3.07 and we therefore included all diffraction data to 1.4 Å resolution in the refinement to increase the data-to-parameter ratio. The full statistics for all shells are given in the supplementary table[1] and the effective resolution was estimated to be 1.7 Å by analyzing the amplitudes of the observed structure factors (Swanson, 1988). A total of 15 039 independent reflections were obtained with an overall $R_{\rm merge}$ of 8.6% from 31 649 observed reflections. A randomly selected 5% of reflections were assigned as a test set for cross-validation. Refinement was carried out using the program *CNS* v.1.1 (Brünger *et al.*, 1998), which was modified for neutron diffraction studies (Ostermann *et al.*, 2002; Chatake *et al.*, 2003; Kurihara *et al.*, 2004). The refinement procedure used in this study is as follows: positional minimization and *B*-factor refinement for all atoms was performed and occupancy refinement was then carried out only for the peptide amide H/D atoms to determine the H/D-exchange ratios. The model was fitted to $2F_{\rm o} - F_{\rm c}$ and $F_{\rm o} - F_{\rm c}$ maps using the program *XtalView* (McRee, 1999). These refinement cycles were repeated to obtain the final structure. The X-ray structure of RNase A solved at 1.1 Å resolution (PDB code 1kf4; Berisio *et al.*, 2002) was used as the initial model. After initial refinement, putative non-exchangeable H atoms were added to the initial model. An OMIT map was calculated for each amino-acid residue; exchangeable D atoms were then added to the model if there was nuclear density. The peptide amide H/D

Table 1
Data-collection and refinement statistics for ribonuclease A.

Values in parentheses are for the outermost resolution shell. All data to the 1.4 Å resolution limit were used in structure refinement to increase the data-to-parameter ratio. The effective resolution was estimated as 1.7 Å using the method of Swanson (1988).

Wavelength (Å)	2.6
Temperature (K)	293
Space group	$P2_1$
Unit-cell parameters	
a (Å)	30.38
b (Å)	38.56
c (Å)	53.40
β (°)	105.78
Resolution (Å)	80–1.4 (1.45–1.40)
Total No. of frames	1211
No. of observed reflections	31649
No. of unique reflections	15039
Redundancy	2.1
Completeness (%)	64.0 (19.5†)
Average $I/\sigma(I)$	8.40 (3.07)
$R_{\rm merge}$ (%)	7.1 (20.5)
$R_{\rm cryst}$ (%)	19.5 (33.3)
$R_{\rm free}$ (%)	23.8 (36.8)
No. of non-H atoms	1043
No. of H atoms	783
No. of D atoms	385
No. of DOD molecules	84
No. of water molecules (O form)	8
Ramachandran allowed regions (%)	86.1
Ramachandran additional allowed regions (%)	13.0
Ramachandran generously allowed regions (%)	0.9
Ramachandran disallowed regions (%)	0.0
R.m.s.d. bond lengths (Å)	0.004
R.m.s.d. bond angles (°)	1.2
Average B factors (Å^2)	14.4

† The completeness of the outermost shell is rather low because of geometrical restrictions of the detector and a shortage of experimental time. Full details showing the completeness of each shell are in the supplementary table.

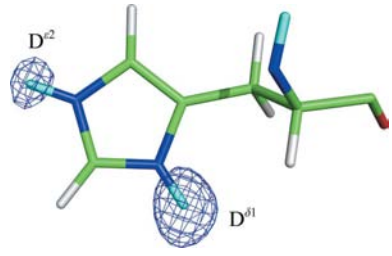

Figure 3
An $|F_{\rm o}| - |F_{\rm c}|$ OMIT map calculated after omission of D$^{\delta 1}$ and D$^{\varepsilon 2}$ from His12. The blue contour shows the 5σ level.

[1] Supplementary material has been deposited in the IUCr electronic archive (Reference: BE5125). Services for accessing this material are described at the back of the journal.

atoms were introduced to the structure as alternate conformations and the occupancy factors were then refined. Afterwards, D_2O molecules were added to the structure if the nuclear density could accommodate them. For small densities, only water O atoms were located. At the end of the refinement, 92 water molecules (84 D_2O, eight O) were included in the model. The protonation states of side chains, orientations of methyl groups and water positions were confirmed by calculating a $2F_o - F_c$ map and an OMIT map for each amino-acid residue and water molecule. The final values of R_{cryst} and R_{free} were 19.5% and 23.8%, respectively, for 15 029 unique reflections to a resolution of 1.4 Å. The coordinates and structure factors have been deposited in the RCSB PDB under accession code 3a1r. All figures representing molecular structures were created using the software *PyMOL* (DeLano, 2002).

3. Results and discussion

3.1. Structure of the active site

We determined the structure of the active site of phosphate-free RNase A using our neutron diffraction experiment. The PO_4 group in the phosphate-bound model is replaced by three water molecules (Wlodawer *et al.*, 1986), DOD41, DOD76 and O89, in the phosphate-free model, as shown in Fig. 2(*b*). In the phosphate-bound model (Fig. 2*a*), O^1 of the phosphate group is hydrogen bonded to $D^{\delta1}$ of His119 and O^2 of the phosphate group is hydrogen bonded to $D^{\varepsilon2}$ of His12. In contrast, in our phosphate-free model these interactions are replaced by hydrogen bonds involving water molecules. The O atom of DOD41 is hydrogen bonded to $D^{\varepsilon2}$ of His12. $D^{\delta1}$ of His119 is hydrogen bonded to O atom O89 (2.4 Å). $D^{\varepsilon2}$ of His119 is hydrogen bonded to $O^{\delta1}$ of Asp121. It was reported that at pH 6.3 the active site contains a sulfate ion which is hydrogen bonded to the ordered His119, whereas at pH 7.1 the active site releases the sulfate ion and contains a disordered His119 (Berisio *et al.*, 1999). Although a soaking solution at pD 6.2 was used in this study, the active site does not contain the phosphate group and His119 is ordered, while DOD37 and DOD39 exist at the location the disordered His119 could have occupied. This difference might arise from the two different crystallization methods. The O atom of DOD41 forms possible hydrogen bonds to D^2 of DOD37, D^1 of DOD3 and O of DOD76. DOD3 is hydrogen bonded to $D^{\varepsilon21}$ of Gln11. DOD3 is one of the most deeply buried water molecules in the pocket of the catalytic site and has a *B* factor of 17.1 $Å^2$, which is lower than those of the other water molecules located at the surface of RNase A. We must point out that the *B* factor of DOD41 is 42.1 $Å^2$, which is higher than those of other water molecules, which have an average value of 29.2 $Å^2$. This suggests that DOD41 could be relatively easily replaced by other substrates. The occupancy of DOD41 may also be affected by the protonation state of His12, a hydrogen-bonding partner (see §3.2).

3.2. Protonation states of His12 and His119

His12 and His119 are located at the catalytic site of RNase A and play important roles in its enzymatic activity (Fig. 1). His12 is known to act as a general base that removes a proton from the RNA 2′-OH group and thereby promotes its nucleophilic attack on the adjacent P atom. On the other hand, His119 is believed to act as general acid, enabling bond scission by protonating the leaving group. To act as a base, His12 should be singly protonated. However, double protonation of His12 at acidic pH had been reported from both X-ray and neutron diffraction analyses (Berisio *et al.*, 1999; Wlodawer *et al.*, 1983; Wlodawer & Sjölin, 1983). Our neutron diffraction analysis indicated that His12 also appears to be doubly protonated (positively charged) at first glance. If that were the case, it would be impossible for His12 to extract a proton from the 2′-OH group of RNA under these conditions. To confirm the protonation state of His12, we calculated an $|F_o| - |F_c|$ nuclear density map after first omitting $D^{\delta1}$ and $D^{\varepsilon2}$ of His12 as shown in Fig. 3. The nuclear density for $D^{\delta1}$ is higher than that for $D^{\varepsilon2}$ at the 5σ level, implying a lower occupancy for $D^{\varepsilon2}$. This result means that a certain proportion of His12 residues have a singly protonated imidazole ring, allowing the proton from the RNA 2′-OH group to be removed at pD 6.2. Our results thus support the hypothesis that His12 is singly protonated part of the time and is capable of acting as a general base in the catalytic mechanism of RNase A.

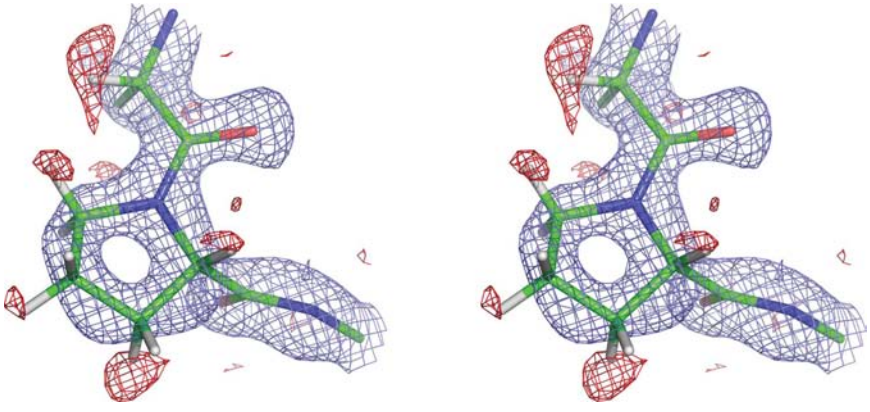

Figure 4
Final $2|F_o| - |F_c|$ neutron-density maps of Pro117. Blue and red contours show the 1.5σ and -2.5σ levels, respectively. H atoms are shown with negative density because of the negative nuclear scattering factor for hydrogen. The clear appearance of a hole in the five-membered rings of the proline residues is an indication of the high-resolution nature of this neutron diffraction analysis.

3.3. How can H, D atoms be observed in neutron protein crystallographic analysis?

RNase A contains 15 serine residues, ten threonine residues and six tyrosine residues. The orientations of all the hydroxyl groups of these residues, except for Ser32, Ser59, Ser77 and Tyr73, were determined from nuclear density maps and these orientations

are all well explained by the formation of hydrogen bonds. It is noteworthy that the orientations of 24 of the 31 hydroxyl groups are different from the results reported in a previous neutron diffraction analysis (Wlodawer, 1980).

RNase A contains four proline residues. It was rather difficult in the earlier medium-resolution neutron diffraction experiment to observe the detailed puckering conformation of the proline rings, but in our present high-resolution neutron diffraction study the five-membered rings of three proline residues (Pro42, Pro93, Pro117) were observed clearly. The $2|F_o| - |F_c|$ map of Pro117 is shown in Fig. 4 as an example.

The neutron scattering length of a D atom is comparable to those of other non-H atoms; thus, the nuclear density of an ND_2 group (three atoms) expands to about three times the area of an O atom (one atom). Therefore, the two ends of the amide side chains ($COND_2$) of asparagine and glutamine residues (*i.e.* ND_2 *versus* O) are completely distinguishable in neutron maps. RNase A contains ten asparagine and seven glutamine residues and almost all of the ordered amide side chains ($COND_2$) of the asparagine and glutamine residues could be unambiguously observed correctly; those of Asn24, Asn113 and Gln28 residues were exceptions because of their disordered conformations. In medium-resolution X-ray crystallographic analyses of proteins it is very difficult to distinguish the NH_2 group from the O atom in an amide group because of the 'near-invisibility' of the H atoms in NH_2 groups to X-rays.

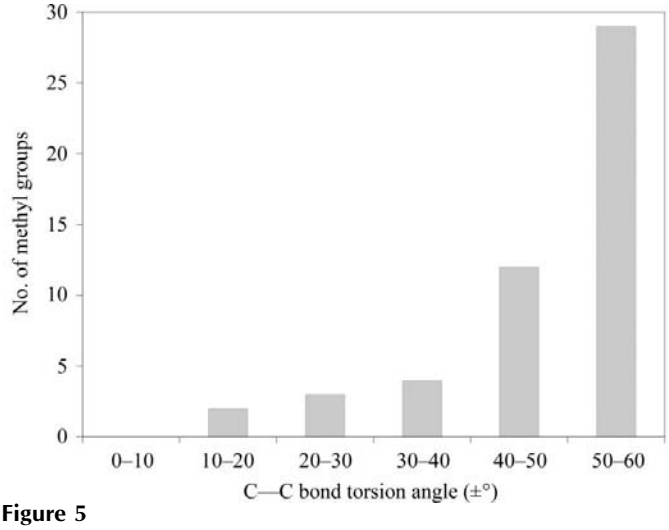

Figure 5
Distribution of the C—C bond torsion angles of the methyl groups in ribonuclease A.

Most methyl groups, including H atoms, of alanine, isoleucine, leucine and valine were clearly observed. There are 50 methyl groups in RNase A and the C—C bond torsion angles of these methyl groups were calculated; the distribution of the torsion angles is shown in Fig. 5. Generally speaking, the C—C bond torsion angle of gaseous ethane is close to 60° (staggered conformation) and those in a protein are expected to have similar values in order to avoid stereochemical repulsion from neighbouring methyl groups. It was found that most methyl groups had staggered conformations (±60°).

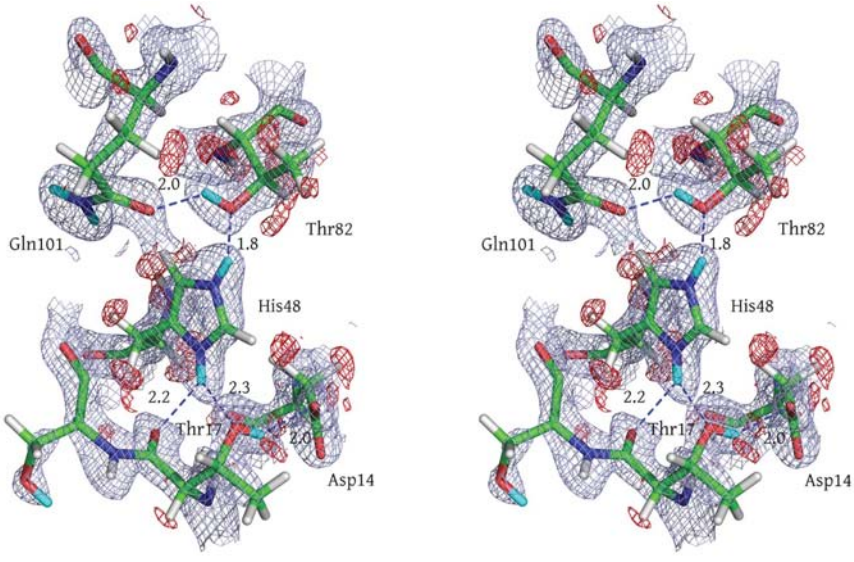

Figure 6
Structure around the His48 residue. Blue and red contours show the1.5σ and −2.5σ levels of the $2|F_o| - |F_c|$ neutron-density map, respectively. Hydrogen bonds are indicated by white broken lines. Gln101 is hydrogen bonded from His48 through the Thr82 residue. Note that His48 is doubly protonated and that one of the two N—H bonds forms a bifurcated hydrogen bond with two O atoms.

Table 2
Protonation states of charged amino-acid side chains.

Residues	Protonation state
Arg10, Arg33, Arg39, Arg85	Protonated
His12, His48, His105, His119	Doubly protonated
Lys7, Lys31, Lys41, Lys104	Protonated
Lys1, Lys37, Lys61, Lys66, Lys91, Lys98	Disordered
Asp14, Asp38, Asp53, Asp83, Asp121	Deprotonated
Glu2, Glu9, Glu49, Glu86, Glu111	Deprotonated

3.4. Protonation and deprotonation states of amino acids

The protonation states of the charged amino acids (Arg, Lys, Asp and Glu) were clearly observed and several distinctive features of each amino acid are discussed below and summarized in Table 2. The pK_a values of glutamic acid and aspartic acid are about 4.3 and 3.9, respectively. All glutamic acid and aspartic acid residues of RNase A were observed to be deprotonated in our neutron results at pD 6.2. RNase A contains ten lysine residues. Generally, it is difficult to observe a sufficient nuclear density of lysine in neutron diffraction experiments, but Lys7 was clearly defined. Six lysines (Lys1, Lys37, Lys61, Lys66, Lys91 and Lys98) did not show sufficient nuclear density because of their disordered conformations. We note that it was previously reported that five lysine residues (Lys1, Lys31, Lys37, Lys41 and Lys91) did not show sufficient nuclear

density in the neutron analysis of RNase A at 2.8 Å resolution (PDB code 5rsa). The pK_a value of lysine is 10.8 and all the lysine residues were found to be protonated as indicated in Table 2, except for the disordered lysine residues (Lys1, Lys37, Lys61, Lys66, Lys91 and Lys98), which were not determined. RNase A contains four histidines (His12, His48, His105 and His119). Our crystal was grown at pD 6.2, which is close to the pK_a value of monoprotonated (neutral) histidine (6.0), but all histidines were found to be doubly protonated (Table 2). It is important to know the protonation states of these residues for the following reasons, some of which were pointed out earlier in this paper: (i) His12 and His119 are strongly expected to play a direct role in enzymatic reactions depending on their protonation and/or deprotonation states (Fig. 1) and (ii) it has been reported that tilting of the imidazole ring of His48 causes sequential movement of the protein backbone in the region around Gln101 through a hydrogen-bonding network around His48 (Berisio *et al.*, 1999).

3.5. Hydrogen-bonding networks around His48 and Gln101

The details of the hydrogen-bonding network around His48 at various pH values were speculated upon, without knowing the actual positions of the H atoms, in a previous X-ray analysis. This was performed in order to explain the movement of the Gln101 residue at alkaline pH (Berisio *et al.*, 1999). In our neutron diffraction results, we confirmed this speculation by not only determining the H-atom positions but also defining their donor and/or acceptor characteristics (Fig. 6). The $N^{\varepsilon 2}$ atom of the His48 imidazole ring donates a hydrogen bond to $O^{\gamma 1}$ of Thr82 (with an $H\cdots O^{\gamma 1}$ distance of 1.8 Å) and the $O^{\gamma 1}$ atom donates a hydrogen bond to the carbonyl O atom of the Gln101 side chain ($H\cdots O$ distance of 2.0 Å). The $N^{\delta 1}$ atom of the His48 imidazole acts as a donor in a bifurcated manner, donating a hydrogen bond not only to the $O^{\gamma 1}$ atom of Thr17 ($H\cdots O^{\gamma 1}$ distance of 2.3 Å) but also to its backbone carbonyl O atom ($H\cdots O$ distance of 2.2 Å). Finally, the $O^{\gamma 1}$ hydroxyl group of Thr17 acts as a hydrogen-bond donor to the $O^{\delta 2}$ atom of Asp14 ($H\cdots O^{\delta 2}$ distance of 2.0 Å).

3.6. Hydration structure

It has been reported previously that observed water molecules can be categorized into the following classes based on their appearance in Fourier maps: (i) triangular shaped, (i) ellipsoidal stick shaped and (iii) spherical shaped. This classification conveniently reflects the degree of disorder and/or dynamic behaviour of a water molecule; that is, their shapes can also be correlated with their *B* factors (Chatake *et al.*, 2003). In this RNase A structure, the water molecules were assigned as 84 D—O—D-type waters and eight O-type waters. The average *B* factor for the two types were 30.2 and 59.2 Å^2, respectively. The 84 D—O—D-type water molecules can be classified either by their *B* factors or by the number of anchor points, which are defined as the number of atoms of D—O—D involved in hydrogen bonds. For each group, the average hydrogen-bond length was also calculated. These results are shown in Fig. 7, which shows that the water molecules having more anchor points tend to have smaller *B* factors and shorter hydrogen-bond lengths.

3.7. Hydrogen bonds in α-helices and β-sheets

Bovine pancreatic RNase A contains three α-helices and two β-sheets. In our neutron study, the average hydrogen-bond lengths within the α-helices and in the β-sheets were 2.2 ± 0.2 and 2.0 ± 0.2 Å, respectively, where the hydrogen-bond length is defined as the $H\cdots O$ distance in the backbone $N-H\cdots O{=}C$ interaction. From these values, it could be concluded that the hydrogen bonds in β-sheets might be stronger than those in α-helices. The hydrogen-bond lengths of α-helices are quite comparable to those determined previously for myoglobin, which has eight α-helices and for which we have also reported the high-resolution neutron structure (1.5 Å resolution). In that study, the average hydrogen-bond lengths of the eight α-helices was also 2.2 ± 0.2 Å (Ostermann *et al.*, 2002).

3.8. H/D exchange in RNase A

The crystal used for our neutron diffraction experiment was soaked in deuterated solution for two months. As a result, the hydrogen/deuterium (H/D) exchange ratios of the amide H atoms of RNase A were obtained as shown in Fig. 8(*a*). There are 35 H atoms that are completely or partially protected from H/D exchange (in other words, those in which the H/D-exchange ratio is less than 0.3, as shown in Fig. 8*a*). It is of interest to compare our results with those from the earlier neutron study (Wlodawer & Sjölin, 1983). The D_2O-soaking periods of our crystals and those of Wlodawer and Sjölin were two months and six months, respectively. According to them, 17 amide H atoms were fully protected and all of these also

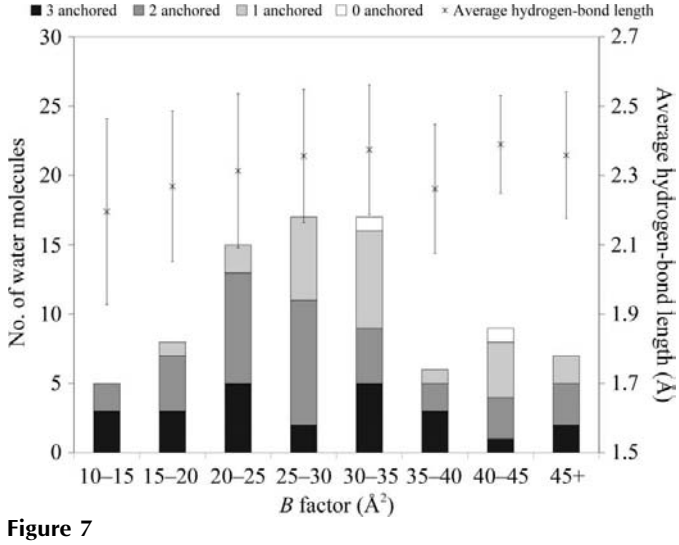

Figure 7
Histogram showing the correlation between the *B* factors and the number of D—O—D molecules. Each histogram bar also shows the number of D—O—D molecules with different anchor points from 0 to 3, which are defined as the number of atoms of D—O—D involved in hydrogen bonds. The dispersion graph (×) shows the correlation between the *B* factors and the average hydrogen-bond lengths in the hydration networks involving D—O—D molecules. The error bars show ±σ.

appear in our list of 35 protected H atoms. Therefore, in terms of soaking time *versus* the H/D-exchange ratio, we can classify the amide H atoms into three categories as shown in Fig. 8(*b*): (i) those H atoms that are fully deuterated after two months (shown as open circles or open rectangles), (ii) those in which H/D exchange occurs between two and six months (lightly shaded shapes) and (iii) those in which amide H atoms are undeuterated even after six months (dark filled shapes).

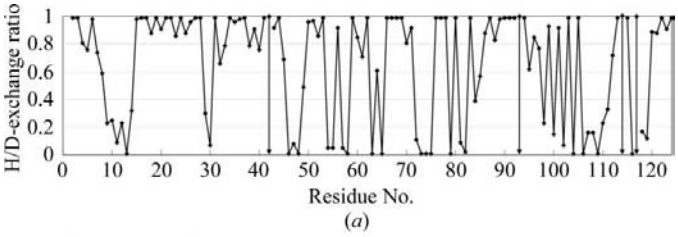

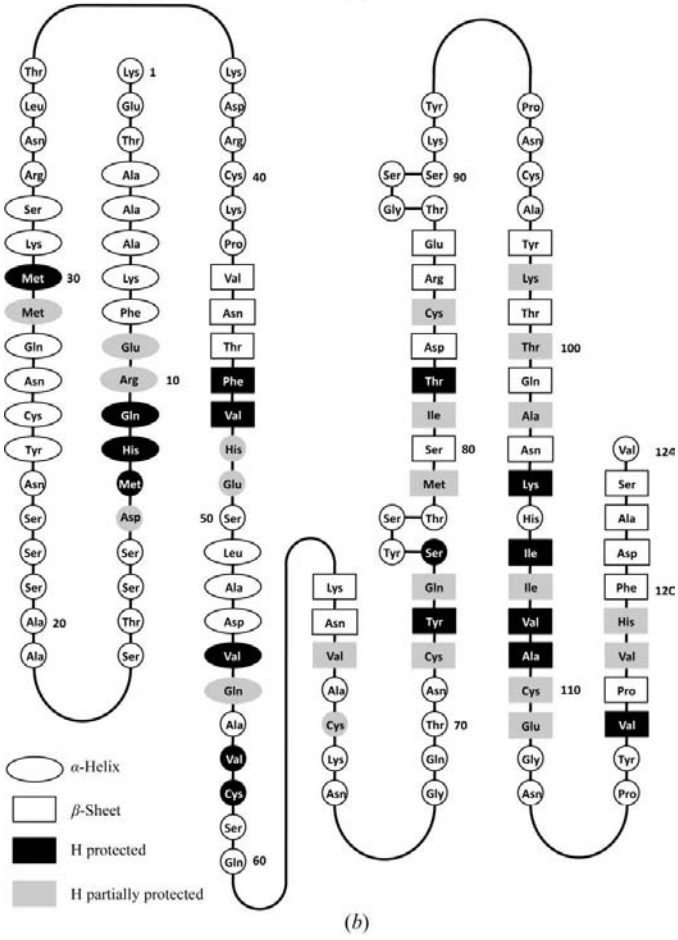

Figure 8
(*a*) H/D-exchange ratios of amide H atoms, in which a value of 1 indicates that a H atom has been replaced by a D atom completely, while a value of 0 corresponds to a H atom that has totally resisted deuteration. Note that the downward-pointing arrows show the proline positions (that is, residues 42, 93, 114 and 117), which do not have any backbone amide H atoms. (*b*) A diagram summarizing the time evolution of H/D exchange of amide H atoms (see text). Here, the ellipses, rectangles and circles indicate amino acids belonging to α-helices, β-sheets and other regions (*e.g.* random loops), respectively. The open shapes, lightly filled shapes and dark filled shapes indicate residues in which deuteration of the N—H groups is complete within two months, in which H/D exchange takes place between two and six months and N—H groups which remain undeuterated even after six months of soaking of the crystals in D_2O, respectively.

We found that the H/D-exchange ratios are different for H atoms in α-helices compared with those in β-sheets. The percentages of amide H atoms which undergo deuterium exchange (after two months of soaking in our study) in α-helices and in β-sheets are 65% and 46%, respectively. In Fig. 8(*b*), amino-acid residues which belong to α-helices, β-sheets and others are indicated by ellipses, rectangles and circles, respectively. This means that the hydrogen bonds of β-sheets are more strongly protected from H/D exchange than those of α-helices. This is consistent with the previous discussion on the strengths of hydrogen bonds in α-helices and β-sheets in terms of hydrogen-bond lengths.

4. Conclusions

The crystal structure of phosphate-free bovine pancreatic ribonuclease A was determined at 1.7 Å resolution using the BIX-4 single-crystal neutron diffractometer at the JRR-3 reactor of the Japan Atomic Energy Agency.

The final values of $R_{\rm work}$ and $R_{\rm free}$ for ribonuclease A were 19.5% and 23.8%, respectively, for 31 649 observed reflections and 15 029 unique reflections with 92 water molecules. The refined structural model allows us to declare that His12 is able to act as a general base in the catalytic process of RNase A by showing that the occupancies of $D^{\delta1}$ and $D^{\varepsilon2}$ of His12 have a significant difference, even though at first glance His12 appeared to be doubly protonated (positively charged).

The conformations of the methyl groups, accurate orientations of virtually all of the hydroxyl groups, puckering details of the five-membered rings of prolines and a clear distinction between the NH_2 and oxygen groups of the amide side chains of asparagine and glutamine could all be determined uniquely at a resolution of 1.7 Å.

The protonation and deprotonation states of the charged amino-acid residues were determined and the neutron results have provided us with valuable information regarding the identities of the donors and acceptors of the hydrogen-bonding network around the active site and at the His48 residue, including the positions of the key H atoms.

The differences in hydrogen-bonding strengths between α-helices and β-sheets could be estimated from the average hydrogen-bond lengths as well as from the H/D-exchange ratios of the amide H atoms of the polypeptide backbone.

The differences in the H/D-exchange ratios of the amide H atoms as a function of time (two-month *versus* six-month soaks in D_2O) were measured; from them, three different categories of H/D-exchange characteristics could be classified.

We are grateful to Professor R. Bau for reading the manuscript and providing criticism and advice. We are very sorry that Professor R. Bau passed away on 28 December 2008. We thank Professor H. Yamada for the valuable discussion on the catalytic mechanism of RNase A. This work was supported in part by a 'Grant-in-Aid for Scientific

Research B' from the Ministry of Education, Culture, Sports, Science and Technology of Japan and from a Research Grant funded by the Human Frontier Science Program.

References

Avey, H. P., Boles, M. O., Carlisle, C. H., Evans, S. A., Morris, S. J., Palmer, R. A., Woolhouse, B. A. & Shall, S. (1967). *Nature (London)*, **213**, 557–562.

Berisio, R., Lamzin, V. S., Sica, F., Wilson, K. S., Zagari, A. & Mazzarella, L. (1999). *J. Mol. Biol.* **292**, 845–854.

Berisio, R., Sica, F., Lamzin, V. S., Wilson, K. S., Zagari, A. & Mazzarella, L. (2002). *Acta Cryst.* D**58**, 441–450.

Brünger, A. T., Adams, P. D., Clore, G. M., DeLano, W. L., Gros, P., Grosse-Kunstleve, R. W., Jiang, J.-S., Kuszewski, J., Nilges, M., Pannu, N. S., Read, R. J., Rice, L. M., Simonson, T. & Warren, G. L. (1998). *Acta Cryst.* D**54**, 905–921.

Chatake, T., Ostermann, A., Kurihara, K., Parak, G. F. & Niimura, N. (2003). *Proteins*, **50**, 516–523.

DeLano, W. L. (2002). *The PyMOL Molecular Graphics System.* DeLano Scientific LLC, San Carlos, California, USA. http://www.pymol.org.

Findley, D., Herries, D. G., Mathias, A. P., Rabin, B. R. & Ross, C. A. (1961). *Nature (London)*, **190**, 781–784.

Findley, D., Herries, D. G., Mathias, A. P., Rabin, B. R. & Ross, C. A. (1962). *Biochem. J.* **85**, 152–153.

Kurihara, K., Tanaka, I., Chatake, T., Adams, M. W. W., Jenney, F. E. Jr, Moiseeva, N., Bau, R. & Niimura, N. (2004). *Proc. Natl Acad. Sci. USA*, **101**, 11215–11220.

Lindquist, R. N., Lynn, J. L. Jr. & Lienhard, G. E. (1973). *J. Am. Chem. Soc.* **95**, 8762–8768.

McRee, D. E. (1999). *J. Struct. Biol.* **125**, 156–165.

Niimura, N., Arai, S., Kurihara, K., Chatake, T., Tanaka, I. & Bau, R. (2006). *Cell. Mol. Life Sci.* **63**, 285–300.

Niimura, N., Karasawa, Y., Tanaka, I., Miyahara, J., Takahashi, K., Saito, H., Koizumi, S. & Hidaka, M. (1994). *Nucl. Instrum. Methods Phys. Res. A*, **349**, 521–525.

Ostermann, A., Tanaka, I., Engler, N., Niimura, N. & Parak, F. G. (2002). *Biophys. Chem.* **95**, 183–193.

Otwinowski, Z. & Minor, W. (1997). *Methods Enzymol.* **276**, 307–326.

Park, C., Schultz, L. W. & Raines, R. T. (2001). *Biochemistry*, **40**, 4949–4956.

Swanson, S. M. (1988). *Acta Cryst.* A**44**, 437–442.

Tanaka, I., Kurihara, K., Chatake, T. & Niimura, N. (2002). *J. Appl. Cryst.* **35**, 34–40.

Tanaka, I., Niimura, N. & Mikula, P. (1999). *J. Appl. Cryst.* **32**, 525–529.

Usher, D. A., Erenrich, E. S. & Eckstein, F. (1972). *Proc. Natl Acad. Sci. USA*, **69**, 115–118.

Wlodawer, A. (1980). *Acta Cryst.* B**36**, 1826–1831.

Wlodawer, A., Borkakoti, N., Moss, D. S. & Howlin, B. (1986). *Acta Cryst.* B**42**, 379–387.

Wlodawer, A., Miller, M. & Sjölin, L. (1983). *Proc. Natl Acad. Sci. USA*, **80**, 3628–3631.

Wlodawer, A. & Sjölin, L. (1983). *Biochemistry*, **22**, 2720–2728.